Polymer 49 (2008) 4695–4702

Contents lists available at ScienceDirect

Polymer

journal homepage: www.elsevier.com/locate/polymer

Dynamics in complex systems: Dendrimer–polymer blends in electric and mechanical fields

Sanja Ristić, Jovan Mijović*

Othmer–Jacobs Department of Chemical and Biological Engineering, Polytechnic Institute of New York University, Six Metrotech Center, Brooklyn, NY 11201, USA

ARTICLE INFO

Article history:
Received 9 July 2008
Received in revised form 11 August 2008
Accepted 16 August 2008
Available online 27 August 2008

Keywords:
PAMAM dendrimers
Blends
Dynamics

ABSTRACT

An investigation was carried out on the molecular dynamics of blends composed of poly(amidoamine) (PAMAM) dendrimers with ethylenediamine core and amino surface groups (generations 0 and 3) and three linear polymers: poly(propylene oxide) – PPO and two block copolymers, poly(propylene oxide)/poly(ethylene oxide) – PPO/PEO with different mole ratios: 29/6 (amorphous) and 10/31 (crystalline). The results were generated over a broad range of frequency and temperature by Dielectric Relaxation Spectroscopy (DRS) and Dynamic Mechanical Spectroscopy (DMS). Dielectric spectra of dendrimers in the PPO matrix reveal a decrease in the time scale of normal and segmental relaxation with increasing dendrimer concentration. In the amorphous blends with 29PPO/6PEO matrix, no effect of concentration on the time scale of normal and segmental processes was observed. But in the crystalline blends with 10PPO/31PEO matrix, relaxation time increases with increasing dendrimer concentration. Results acquired by DRS and DMS were contrasted and the obtained relaxation times were found to be in excellent agreement. A detailed analysis of the effect of generation and concentration of dendrimers, hydrophilicity and morphology of the polymer matrix and temperature on the molecular origin, the shape of the relaxation spectra, the dielectric relaxation strength and the frequency location for the maximum loss in dendrimer–polymer blends is provided.

1. Introduction

Dendrimers – also known as starburst or cauliflower polymers – represent an exciting and promising novel class of macromolecular architecture [1–3]. First synthesized three decades ago [4–8], their well defined and highly branched compartmentalized structure in the nanometer size range has made them excellent candidates for many applications, including imaging [9,10], sensing [11], optoelectronics [12] and catalysis [13]. Lately, dendrimers have been intensively investigated for applications in gene therapy and drug delivery, as described in several reviews [14–16]. The globular morphology of these polymers lends itself favorably to encapsulation of important molecules, such as therapeutic drugs, within the interstitial space of their branches for subsequent targeted delivery. To understand and assess the potential and to optimize the function of dendrimers for specific tasks in complex environments, such as *in vivo* targeting, it is essential to acquire a comprehensive knowledge of the molecular motions that underlie the physical response of these materials to applied external fields. Further, it is important to understand how dendrimer dynamics are affected by interactions with molecules with various physicochemical properties that are present in complex media such as, for example, the blood stream.

Despite an extensive volume of research on dendrimers, published reports on their molecular dynamics are scarce. Dendrimers have been investigated by dynamic mechanical spectroscopy (DMS), but that study was limited to a narrow frequency range [17]. Among available experimental techniques for the study of molecular dynamics, dielectric relaxation spectroscopy (DRS) is rapidly becoming a dominant tool [18,19], because of its unparalleled frequency range of up to 16 decades. That feature of DRS enables one to capture molecular dynamics over a broad range of time scales and length scales. DRS has been employed to study phosphorus-containing dendrimers [20–22] and carbosilane dendrimers with perfluorinated [23] and cyanobiphenyl [24] end groups. A common finding in those studies is that dendrimers exhibit typical relaxation characteristics of glass forming materials. More recently, we have performed a comprehensive study of the dynamics of six generations of PAMAM dendrimers over a broad range of temperature and frequency. One interesting result was that molecular dynamics are affected by the interplay between molecular structure and hydrogen bonding [25].

The above described studies were limited to neat dendrimers and it is now of interest to probe their dynamics in complex media.

* Corresponding author. Tel.: +1 718 2603097; fax: +1 718 2603125.
E-mail address: jmijovic@poly.edu (J. Mijović).

0032-3861/$ – see front matter © 2008 Elsevier Ltd. All rights reserved.
doi:10.1016/j.polymer.2008.08.039

To that end we herein report on a study of dynamics of blends composed of generation 0 or 3 PAMAM dendrimer and a polymer matrix. We note that, while generation 3 is by definition a dendrimer, generation 0 is not fully developed and does not possess a globular morphology. By controlling the composition and properties of dendrimers and polymers in the blend we aim at creating a complex environment with desired properties. The principal objective of this study is to conduct a systematic investigation of blends of PAMAM dendrimers and linear polymers, evaluate the effect of hydrophilicity and morphology of the polymer matrix and quantify the effect of molecular and external factors on blend dynamics. Knowledge of dynamics enables one to tailor macroscopic behavior from nanoscopic concepts. To the best of our knowledge this study marks the first published report on the dynamics of PAMAM dendrimer–polymer blends as studied by DRS and DMS.

2. Experimental section

2.1. Materials

Generations 0 and 3 of poly(amidoamine) – PAMAM dendrimers with ethylenediamine core and amino surface groups in methanol solution (20 wt%) were obtained from Aldrich. Poly(propylene oxide) – PPO with symmetrical dipole inversion was acquired from Bayer, while the two poly(propylene oxide)/poly(ethylene oxide) – PPO/PEO block copolymers were obtained from Huntsman. The block copolymers have PPO/PEO mole ratios of 29/6 and 10/31 and are referred to as 29PPO/6PEO and 10PPO/31PEO, respectively. The average molecular weight of all three polymers is $M_n = 2000$ g/mol. Blends were prepared by mixing the desired amounts of dendrimer and polymer in methanol using a high speed stirrer. Samples were then placed in a vacuum oven for 7 days, in order to remove the solvent completely. All investigated samples and their codes are summarized in Table 1. In the sample code, the first two symbols define the dendrimer generation (G0 or G3). The following number describes the weight percent of dendrimer in the blend, and the last segment in the code describes the polymer matrix. For example, G0 18% – 29PPO/6PEO represents a blend of PAMAM dendrimers of generation 0 at 18% weight fraction with 29/6 PPO/PEO block copolymer.

Table 1
Investigated samples

Description	Wt% of dendrimers in linear neat and block copolymer matrix (G0/G3)	Code
G0 + PPO	2	G0 2% – PPO
G0 + PPO	5	G0 5% – PPO
G0 + PPO	7	G0 7% – PPO
G0 + PPO	10	G0 10% – PPO
G0 + PPO	15	G0 15% – PPO
G3 + PPO	5	G3 5% – PPO
G3 + PPO	10	G3 10% – PPO
G3 + PPO	18	G3 18% – PPO
G3 + PPO	30	G3 30% – PPO
G0 + 29PPO/6PEO	10	G0 10% – 29PPO/6PEO
G0 + 29PPO/6PEO	18	G0 18% – 29PPO/6PEO
G3 + 29PPO/6PEO	10	G3 10% – 29PPO/6PEO
G3 + 29PPO/6PEO	18	G3 18% – 29PPO/6PEO
G3 + 29PPO/6PEO	30	G3 30% – 29PPO/6PEO
G0 + 10PPO/31PEO	5	G0 5% – 10PPO/31PEO
G0 + 10PPO/31PEO	10	G0 10% – 10PPO/31PEO
G0 + 10PPO/31PEO	30	G0 30% – 10PPO/31PEO
G3 + 10PPO/31PEO	5	G3 5% – 10PPO/31PEO
G3 + 10PPO/31PEO	10	G3 10% – 10PPO/31PEO
G3 + 10PPO/31PEO	30	G3 30% – 10PPO/31PEO

2.2. Techniques

The glass transition and the melting temperature were determined by Differential Scanning Calorimetry (DSC) using a TA Instrument Co. modulated DSC model Q2000. Samples were first cooled to 183 K and then heated at 10 K/min to 373 K. For dielectric measurements, samples were placed between two aluminum electrodes, 12 mm in diameter and with 50 μm spacing between them. All dielectric measurements were performed in the frequency range from 10^{-1} Hz to 10^{6} Hz using Novocontrol α Analyzer, interfaced to computers via IEEE 488.2 and connected to a heating/cooling unit (modified Novocontrol Novocool System), that can control temperature from 173 K to 523 K with a precision of ±0.5 K. Further details about our experimental facility for dielectric measurements are given elsewhere [26]. Mechanical measurements were conducted in the frequency range from 0.1 rad/s to 100 rad/s using a Rheometric Scientific's Advanced Rheometric Expansion System (ARES) rheometer. Parallel plate geometry was employed with a typical gap between the plates of 0.5–1.5 mm. Values for the strain were adjusted from 0.2% to 25% for the measurable torque in the linear viscoelastic range.

3. Results and discussion

This section is organized as follows: we begin our discussion by examining the relaxation dynamics of all individual components and then proceed with the analysis of a series of blends composed of PAMAM dendrimers and each of the three linear polymers as matrix.

3.1. Individual components

3.1.1. PAMAM dendrimers

We recently reported on the molecular dynamics of the first six (zero through five) generations of PAMAM dendrimers [25], and hence our goal here is not to be comprehensive. Nonetheless, we will briefly summarize findings relevant to this study. The dynamics of PAMAM dendrimers are significantly different below and above their calorimetric T_g which is located around 243 K. Below this temperature, three local relaxation processes were observed in all generations: β, γ and δ, in the order of increasing frequency at constant temperature. All of these processes are characterized by symmetric, Cole–Cole type relaxation spectra and an Arrhenius-like temperature dependence of the average relaxation time. Moreover, they shift to higher frequency and increase in intensity with increasing temperature. The slowest process in this temperature range, the β process, is assigned to the local fluctuations of branch ends which include amino groups. The process with intermediate time scale (γ) was affected by the interplay between molecular architecture and hydrogen bonding and is attributed to the motions of the amide groups that are not hydrogen bonded to the neighboring chains. It was explained that in generations 0 through 2, hydrogen bonding occurs predominantly between amide groups on two different molecules (hence *inter*molecularly), while in generations 3–5, *inter*molecular hydrogen bonding is replaced with *intra*molecular hydrogen bonding. The origin of the fastest process (the δ process) lies in the motions of amino groups on the surface of dendrimers.

Although dynamics above 253 K were not investigated in the present study, we note that in this range all dendrimers are characterized by a pronounced dielectric modulus peak characteristic of the α process in glass formers. This process shifts to higher frequency and decreases in intensity with increasing temperature. The temperature dependence of the average relaxation time of this process is of the Vogel–Fulcher–Tammann (VFT) type.

3.1.2. Neat PPO and PPO/PEO block copolymers

Dielectric and mechanical properties of neat polymers and block copolymers have been investigated by various groups [27,28], and we will briefly summarize our findings on PPO and the two block copolymers used herein as a necessary prerequisite for the discussion of the dynamics of their blends.

First, we state the characteristic thermal transitions. PPO and 29PPO/6PEO are amorphous polymers with glass transition temperature of 204 K and 199 K, respectively. 10PPO/31PEO block copolymer is crystalline, with an estimated (from the heat of fusion) degree of crystallinity of 28%, T_g of 196 K and T_m of 290 K. The summary of all characteristic thermal transitions is given in Table 2.

Dielectric properties are examined next. Fig. 1 shows dielectric loss in the frequency domain for the following polymers: PPO (Fig. 1A), 29PPO/6PEO (Fig. 1B) and 10PPO/31PEO (Fig. 1C). The solid lines in these figures are the combined fits of the sum of ionic conductivity and the Havriliak–Negami (HN) functional form [29]:

$$\varepsilon^*(\omega) = \varepsilon' - i\varepsilon'' = -i\left(\frac{\sigma_c}{\varepsilon_0\omega}\right)^N + \sum_{k=1}^{n}\left[\frac{\Delta\varepsilon_k}{\left(1+(i\omega\tau_k)^{a_k}\right)^{b_k}} + \varepsilon_{\infty k}\right] \quad (1)$$

where ε_0 is the vacuum permittivity, σ_c is the conductivity, a and b are the shape parameters that define the breadth and the symmetry of the spectrum, respectively, and τ is the average relaxation time.

PPO, a hydrophobic polymer, exhibits two relaxation processes in the temperature range between 203 K and 253 K, and their locations are indicated with arrows in the figure. In addition to the transverse dipole moment that gives rise to the segmental process (α_S), this polymer possesses a persistent cumulative dipole moment along the chain contour which relaxes via the global chain motion (α_N) [30] and, therefore, relaxation of entire chains can be detected. Both processes shift to higher frequency, decrease in intensity with increasing temperature and remain thermodielectrically simple over the investigated temperature range. Additional information about the PPO dynamics can be found elsewhere [30,31].

29PPO/6PEO also exhibits two processes, α_N and α_S, which shift to higher frequency and decrease in intensity with increasing temperature. However, these two processes become more separated with the introduction of a hydrophilic PEO block. The normal mode process becomes slower and the segmental process becomes faster in comparison with the same processes in the neat PPO, and we shall revert to this phenomenon later in the text. The segmental process encompasses the cooperative motions in both PPO and PEO, while the normal mode originates only from the PPO block in the copolymer, since PEO is not a type A polymer in the Stockmayer classification [32] (i.e., it does not have a dipole component parallel to the chain contour).

In this temperature range, 10PPO/31PEO shows only one relaxation process, termed α_A, whose molecular origin lies in the segmental motions within the amorphous phase. With increasing temperature this process shifts to higher frequency and increases in intensity, which is in good agreement with the previous results for segmental motions in the amorphous phase of crystalline polymers [33,34].

The results of dynamic mechanical spectroscopy (DMS) are examined next. Fig. 2 shows storage (G') modulus in the frequency domain, with temperature as a parameter, for (A) PPO and (B)

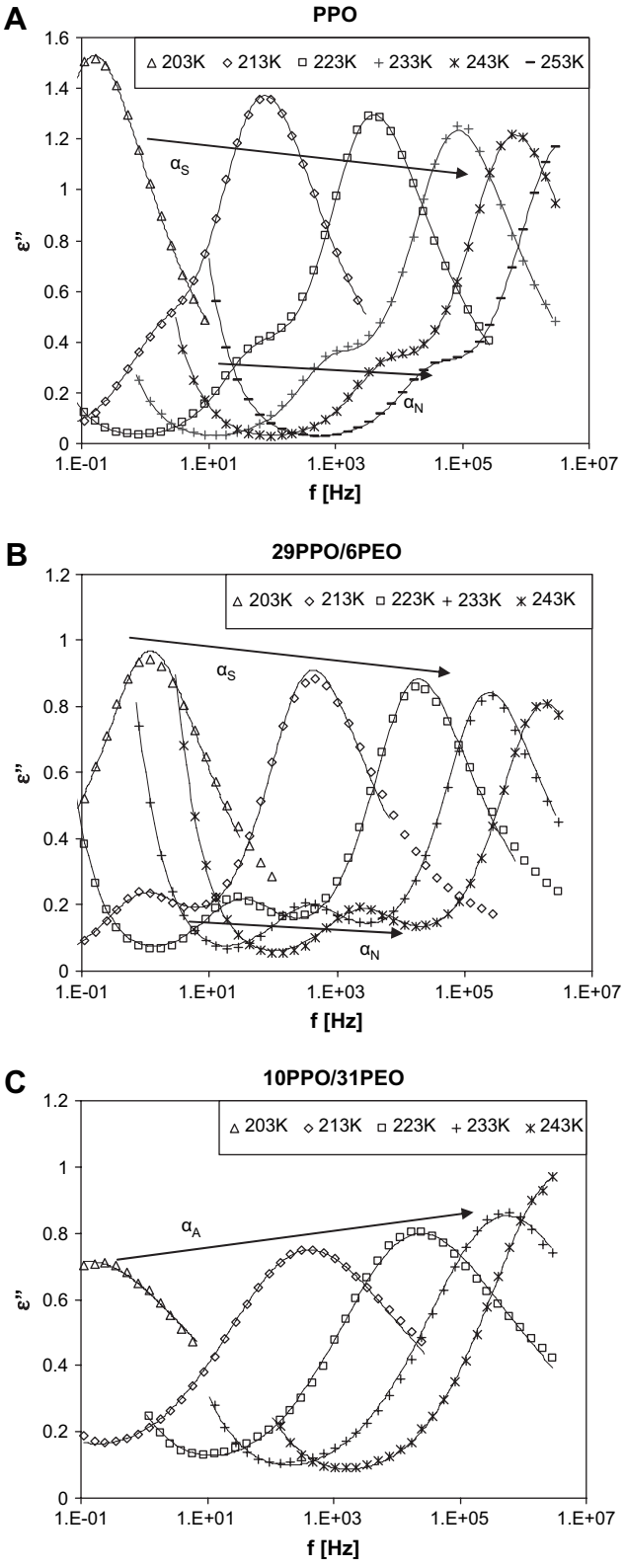

Fig. 1. Dielectric loss in the frequency domain with temperature as a parameter for A – PPO, B – 29PPO/6PEO and C – 10PPO/31PEO.

Table 2
Characteristic thermal transitions of PPO, 29PPO/6PEO and 10PEO/31PPO

Polymer	Composition		T_g (K)	T_m (K)
	x	y		
PPO	35	0	204	–
29PPO/6PEO	29	6	199	–
10PPO/31PEO	10	31	196	290

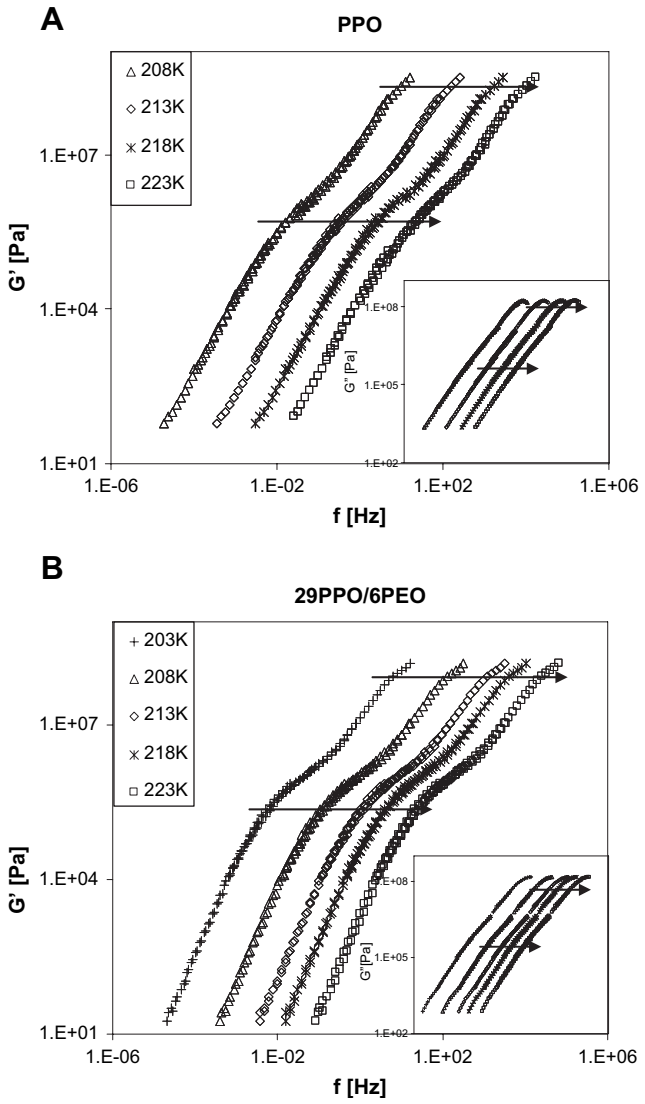

Fig. 2. Storage (G') and loss (G'') moduli in the frequency domain with temperature as a parameter for A – PPO and B – 29PPO/6PEO.

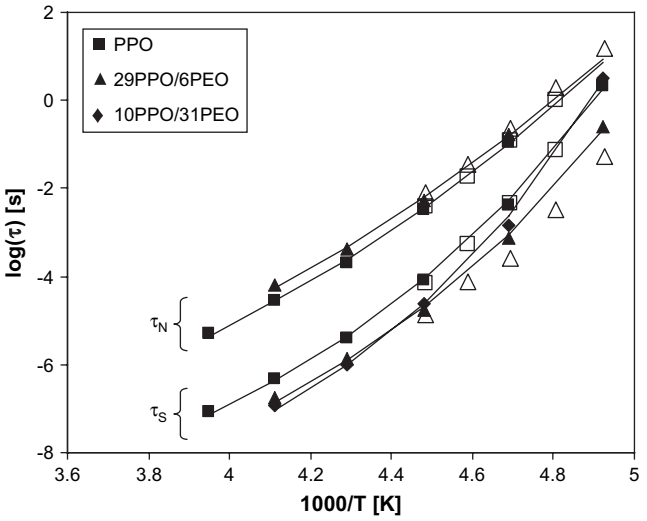

Fig. 3. Average relaxation time as a function of reciprocal temperature for normal and segmental relaxations in neat PPO and block copolymers. Solid symbols represent the DRS results and the open symbols the DMS results.

29PPO/6PEO. Loss (G'') modulus is shown in the inset in these figures. The results shown depict the time–temperature superposed master curves constructed using only the horizontal shift factors. For both polymers we observe segmental and terminal relaxations as indicated by arrows in the figures.

The temperature dependence of the average relaxation time, obtained from the HN fits, was examined next and the results are plotted in Fig. 3. To afford a direct comparison of relaxation times for the normal mode in PPO, we had to divide the DMS τ_N by a factor of two. This is because the longest viscoelastic relaxation time of the Rouse chain is one-half the longest dielectric relaxation time and twice the second dielectric normal mode, which is experimentally measured in samples with symmetrically inverted dipoles [30]. The difference between DMS and DRS relaxation times for the segmental process in 29PPO/6PEO is due to the different nature of dielectric and viscoelastic relaxations of the PEO block. Apart from that, an excellent agreement between the results obtained with these two techniques is evident. The solid lines in Fig. 3 are the VFT fits, whose parameters are summarized in Table 3. As seen in Fig. 3, the addition of hydrophilic PEO slows down the normal mode process in 29PPO/6PEO, about 35% in comparison with the neat PPO. The molecular weight of PPO in the block copolymer is lower than that of the neat PPO and one would intuitively expect a faster process in the former (the length scale and the time scale are directly proportional). However, our results show the opposite trend. To explain that, we envision the following topological picture. Although the neat PPO chains with molecular weight of around 2000 are not in the entangled regime [35,36], the addition of an incompatible PEO block forces an effective elongation, or stretching, of the PPO chains, giving rise to an increased end-to-end distance and consequently a longer relaxation time. Interesting behavior was observed for the segmental process too. The addition of PEO decreases the time scale of the segmental process in 29PPO/6PEO in comparison with the neat PPO and this is in agreement with the DSC results. In the semi-crystalline 10PPO/31PEO however, segmental relaxation is restricted by the PEO crystals, resulting in a different Vogel temperature.

3.2. Blends

We proceed with the analysis of blend dynamics by describing the DRS results first. We focus on the key parameters that define dynamics, namely the real and imaginary parts of dielectric permittivity, the shape of the relaxation spectra, the dielectric relaxation strength, the frequency location for the maximum loss and the temperature dependence of the average relaxation time. We then present the DMS results and compare dielectric and viscoelastic relaxations.

3.2.1. Dielectric relaxation spectroscopy (DRS)

We start by describing the results of PAMAM–PPO blends. The effect of concentration (wt%) of generation 3 in the blend on the dielectric loss in the frequency domain at 233 K is presented in Fig. 4. Two processes seen in the neat PPO are also observed in the blends. Spectra generated at different temperatures show a similar

Table 3
VFT parameters for normal and segmental processes in polymers

Material	Normal mode process			Segmental process		
	τ_0 (s)	B (K)	T_v (K)	τ_0 (s)	B (K)	T_v (K)
PPO	1.0×10^{-14}	2377	134	1.0×10^{-14}	1513	157
29PPO/6PEO	1.0×10^{-14}	2581	128	1.0×10^{-14}	1423	157
10PPO/31PEO	–	–	–	1.0×10^{-14}	1234	166

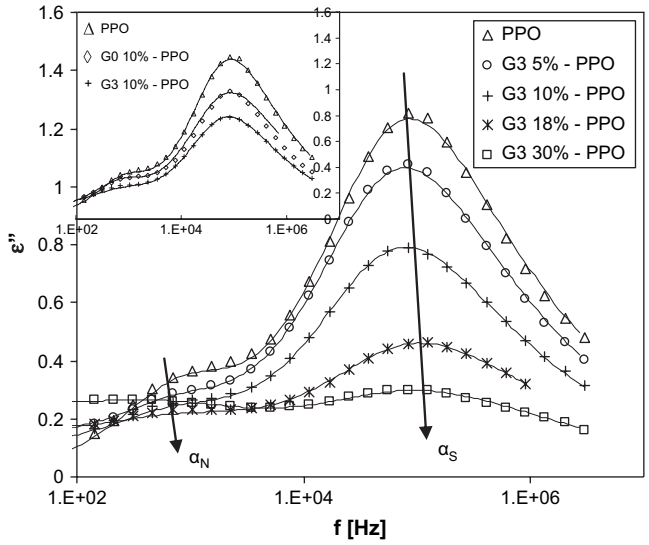

Fig. 4. Dielectric loss in the frequency domain with G3 concentration as a parameter for PAMAM–PPO blends at 233 K. The inset shows the comparison of blends with G0 and G3 for the same concentration of 10% in PPO.

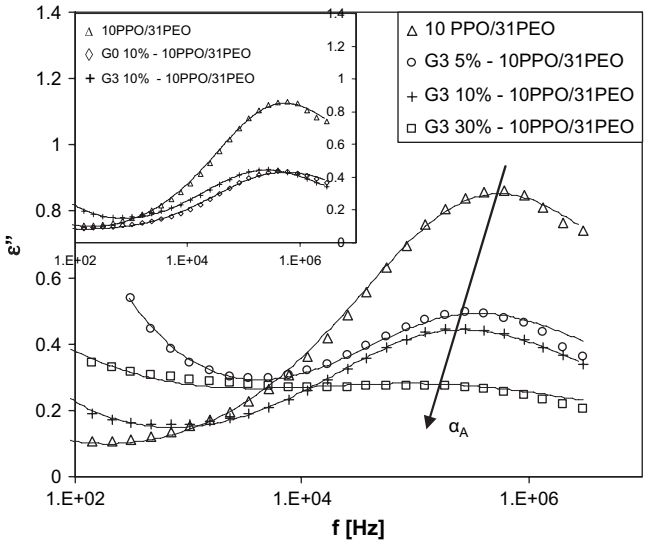

Fig. 6. Dielectric loss in the frequency domain with G3 concentration as a parameter for PAMAM–10PPO/31PEO blends at 233 K. The inset shows the comparison of blends with G0 and G3 for the same concentration of 10% in 10PPO/31PEO.

trend: we observe a slight shift of normal mode and segmental processes to higher frequency with increasing concentration. The peak intensity for segmental and normal mode processes decreases with increasing dendrimer concentration and we shall revert to this observation shortly. Comparison of results obtained for blends that contain generation 0 or 3 PAMAM is shown in the inset of Fig. 4. It is apparent that the peak intensity is higher for the blend with generation 0.

Results for the PAMAM–29PPO/6PEO blends are consider next. Dielectric loss in the frequency domain at 233 K, with concentration of generation 3 dendrimer as a parameter, is presented in Fig. 5. Here, too, the processes seen in the block copolymer are also present in the blend. No change in the time scale of the segmental or normal mode process is observed, but the intensity of the segmental process decreases, while that of the normal mode process increases with increasing dendrimer concentration. The inset in Fig. 5 compares the results for blends with the same concentration (10 wt%) of generations 0 and 3. It can be seen that the intensity of the segmental process for blends with generations 0 and 3 follows the same trend, i.e., the peak intensity decreases with increasing dendrimer concentration. However, the intensity of the normal mode process does not change with the concentration of generation 0 dendrimer.

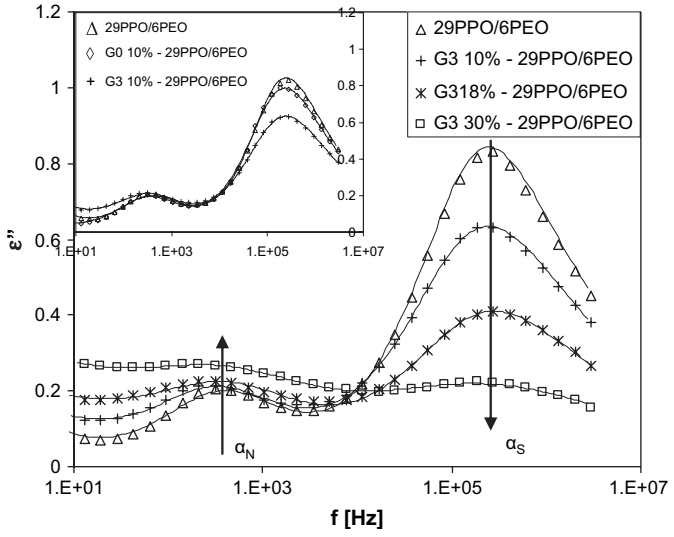

Fig. 5. Dielectric loss in the frequency domain with G3 concentration as a parameter for PAMAM–29PPO/6PEO blends at 233 K. The inset shows the comparison of blends with G0 and G3 for the same concentration of 10% in 29PPO/6PEO.

Next, we examine the PAMAM–10PPO/31PEO blends. Fig. 6 shows dielectric loss in the frequency domain with concentration of generation 3 as a parameter at 233 K. It is evident that the segmental process shifts to lower frequency and decreases in intensity with increasing concentration. Results for the neat 10PPO/31PEO and its blends with generations 0 and 3 at the same concentration (10 wt%) are shown in the inset of Fig. 6. Generation number does not affect the peak intensity in these blends. However, the time scale of segmental process increases with increasing generation number.

The shape of the relaxation spectra is determined by evaluating the HN parameters *a* and *b* which describe the breadth and the symmetry of the spectrum, respectively. These parameters are summarized in Tables 4 and 5. The HN parameters for the normal mode process in blends with generation 0 do not change with dendrimer concentration. However, in blends with generation 3 with PPO or 29PPO/6PEO matrix, parameter *a* decreases with

Table 4
HN parameters for spectral breadth (*a*) and symmetry (*b*)

		PPO				29PPO/6PEO				10PPO/31PEO	
		Normal		Segmental		Normal		Segmental		Segmental	
	Conc	*a*	*b*	*a*	*b*	*a*	*b*	*a*	*b*	*a*	*b*
G0	0	0.90	1	0.80	0.5	0.80	1	0.82	0.5	*f*(*T*)	0.5
	2	0.90	1	0.79	0.5	–	–	–	–	–	–
	5	0.90	1	0.78	0.5	–	–	–	–	*f*(*T*)	0.5
	7	0.90	1	0.77	0.5	–	–	–	–	–	–
	10	0.90	1	0.76	0.5	0.80	1	0.81	0.5	*f*(*T*)	0.5
	15	0.90	1	0.75	0.5	0.80	1	0.80	0.5	–	–
	30	–	–	–	–	–	–	–	–	*f*(*T*)	0.5
G3	5	0.80	1	0.79	0.5	–	–	–	–	*f*(*T*)	0.5
	10	0.75	1	0.78	0.5	0.77	1	0.76	0.5	*f*(*T*)	0.5
	18	0.67	1	0.73	0.5	0.69	1	0.72	0.5	–	–
	30	0.63	1	0.67	0.5	0.60	1	0.54	0.5	*f*(*T*)	0.5

Table 5
Spectral breadth parameter as a function of temperature for segmental process in PAMAM–10PPO/31PEO blends

	conc\T [K]	203	213	223	233	243
G0	0	0.46	0.49	0.51	0.52	0.57
	5	0.46	0.49	0.51	0.51	0.55
	10	0.45	0.46	0.48	0.50	0.55
	30	0.45	0.47	0.48	0.49	0.50
G3	5	0.47	0.49	0.51	0.53	0.56
	10	0.49	0.49	0.51	0.53	0.54
	30	–	0.36	0.36	0.37	0.38

increasing dendrimer concentration, while parameter *b* remains constant. Further, the normal mode process for all blends is symmetric and well-described with the Cole–Cole equation [37]. Also, the normalized loss spectra show that the normal mode process remains thermodielectrically simple in each blend over the investigated temperature range. On the other hand, the spectra of the segmental process broaden with increasing dendrimer concentration. Segmental process remains thermodielectrically simple in blends with PPO and 29PPO/6PEO. But in blends with 10PPO/31PEO the segmental process becomes narrower with increasing temperature, following the same trend observed for the neat copolymer, as shown in Table 5.

Dielectric relaxation strength ($\Delta\varepsilon$) of the normal ($\Delta\varepsilon_N$) and segmental ($\Delta\varepsilon_S$) processes was examined next. $\Delta\varepsilon$ is proportional to height of the loss peak at maximum and is defined by the relationship $\Delta\varepsilon = \varepsilon'(0) - \varepsilon'(\infty)$ where $\varepsilon'(0)$ and $\varepsilon'(\infty)$ represent the limiting low and high frequency dielectric permittivities, respectively. This parameter is directly proportional to the concentration of dipoles and the mean-squared dipole moment per molecule. The effect of temperature, dendrimer concentration and generation on the dielectric strength was studied and the results are plotted in Fig. 7. The bottom rectangle in Fig. 7 depicts dielectric relaxation strength as a function of temperature, with concentration of the generation 0 dendrimer as a parameter. The three boxes on the top of Fig. 7 show the effect of dendrimer generation (0 vs. 3) on the dielectric strength of blends with three different polymer matrices (from left to right: PPO, 29PPO/6PEO and 10PPO/31PEO). An examination of the trends in the dielectric relaxation strength leads

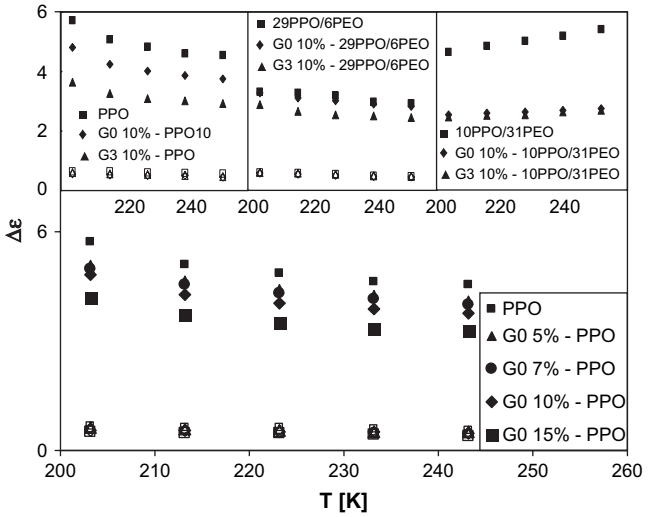

Fig. 7. Bottom: dielectric relaxation strength as a function of temperature with concentration of G0 in PPO matrix as a parameter. Top: dielectric strength as a function of generation in, from left to right, PPO, 29PPO/6PEO and 10PPO/31PEO. Solid symbols represent dielectric relaxation strength for the segmental process and the open symbols for the normal mode process.

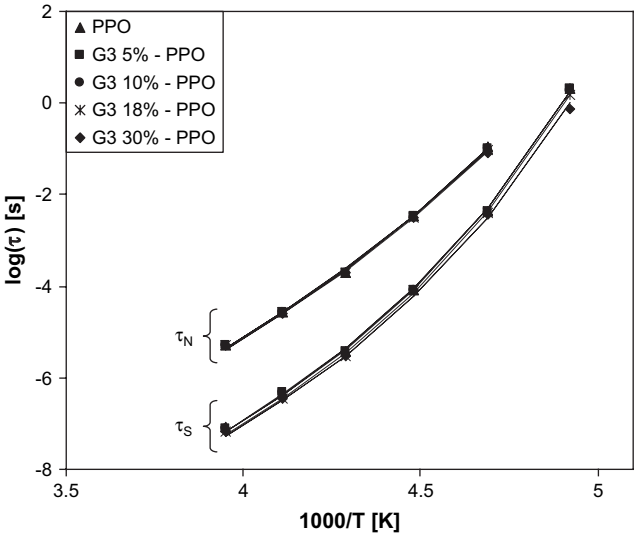

Fig. 8. Average relaxation time as a function of reciprocal temperature for the segmental and normal mode processes for PAMAM–PPO blends with G3 concentration as a parameter.

to the following observations. First, $\Delta\varepsilon_S$ decreases with increasing temperature in PAMAM–PPO and PAMAM–29PPO/6PEO blends, and increases in PAMAM–10PPO/31PEO blend; these are typical characteristics of the segmental process in the amorphous phase of wholly amorphous and semi-crystalline polymers [27,33,34], respectively. Second, $\Delta\varepsilon_S$ decreases with increasing dendrimer concentration. This decrease of dielectric strength is attributed to the interaction of PPO with amino groups on the dendrimer surface. The difference between the dielectric relaxation strength of polymers and blends is greater for the higher generation dendrimer. Although generation 0 has a larger number of amine groups per unit mass, its amide oxygen is more likely to form secondary hydrogen bonds with surface amino groups than in generation 3, where the amide groups are shielded. Further, the difference between the dielectric relaxation strength for blends with generations 0 and 3 diminishes with the reduction of the hydrophobic (PPO) fraction in the polymer (this difference is most pronounced in blends with neat PPO and almost independent of generation number in blends with 10PPO/31PEO). Third, dielectric relaxation strength of the normal mode process is a weak decreasing function of temperature. Fourth, with increasing dendrimer concentration in PPO blends, $\Delta\varepsilon_N$ decreases slightly. And fifth, $\Delta\varepsilon_N$ does not vary with concentration of generation 0 but increases with concentration of generation 3 dendrimers in their blends with 29PPO/6PEO.

Next, we focus our attention to the frequency location of the maximum loss and its temperature dependence, starting with the PAMAM–PPO blends. Fig. 8 shows the average relaxation time for the segmental and normal mode processes, obtained from the HN fits, as a function of temperature and for blends containing generation 3 PAMAM. The solid lines in this figure are the VFT fits, whose parameters are summarized in Table 6. It is interesting to note that

Table 6
VFT parameters for normal and segmental processes in PAMAM–PPO blends

Material	Normal mode process			Segmental process		
	τ_0 (s)	B (K)	T_v (K)	τ_0 (s)	B (K)	T_v (K)
PPO	1.0×10^{-14}	2377	134	1.0×10^{-14}	1513	157
G3 5% – PPO	1.0×10^{-14}	2369	134	1.0×10^{-14}	1510	157
G3 10% – PPO	1.0×10^{-14}	2368	134	1.0×10^{-14}	1506	157
G3 18% – PPO	1.0×10^{-14}	2365	134	1.0×10^{-14}	1491	157
G3 30% – PPO	1.0×10^{-14}	2359	134	1.0×10^{-14}	1486	157

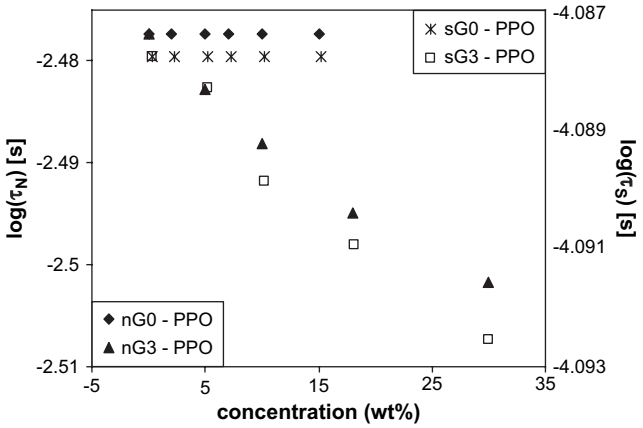

Fig. 9. Average relaxation time for the normal and segmental mode for PAMAM–PPO blends as a function of dendrimers' concentration at 223 K.

the addition of dendrimers has no influence on either the attempt frequency or the Vogel temperature. However, the relaxation time for both normal and segmental mode decreases with increasing dendrimer concentration. Interestingly, the relaxation time does not change in blends with generation 0. This behavior is magnified in Fig. 9 which shows how relaxation time changes with concentration and generation of dendrimers in PAMAM–PPO blends at 223 K. A decrease in relaxation time in generation 3 blends is ascribed to the fact that dendrimers act as hard-sphere diluents in the hydrophobic PPO matrix that decrease the self-association of PPO chains and consequently promote their mobility. It has been shown that this effect varies with the nanoparticles' surface area [38] and that is why it is only observable in blends with generation 3.

In PAMAM–29PPO/6PEO blends we observe no effect of dendrimer concentration on the relaxation time for segmental and normal mode processes and consequently the VFT parameters have the same values as for the neat polymer. This is not surprising because the hydrophobic PPO blocks are already stretched in order to avoid the hydrophilic PEO blocks and the addition of dendrimers is not expected to have an effect on the time scale of relaxations in PEO and PPO.

Finally, the average relaxation time for the PAMAM–10PPO/31PEO blends is obtained and plotted vs. reciprocal temperature

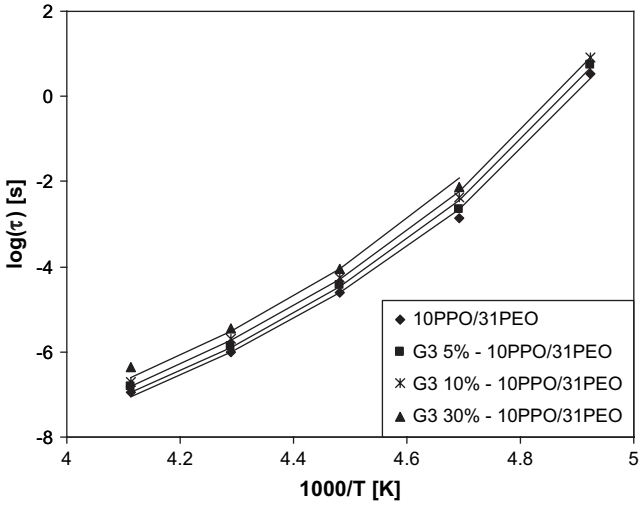

Fig. 10. Average relaxation time as a function of reciprocal temperature for the segmental process in PAMAM–10PPO/31PEO blends with G3 concentration as a parameter.

Table 7
VFT parameters for the segmental process in PAMAM–10PPO/31PEO blends

Material	τ_0 (s)	B (K)	T_v (K)
10PPO/31PEO	1.0×10^{-14}	1234	166
G3 5% – 10PPO/31PEO	1.0×10^{-14}	1255	166
G3 10% – 10PPO/31PEO	1.0×10^{-14}	1277	166
G3 30% – 10PPO/31PEO	1.0×10^{-14}	1311	166

with concentration of generation 3 as a parameter in Fig. 10. VFT parameters are summarized in Table 7. As dendrimer concentration increases, the relaxation time of the segmental process increases too. This behavior is more pronounced in blends with higher generation number, as amplified in Fig. 11, which shows how the average relaxation time changes with dendrimer concentration at 223 K. The observed increase in the time scale of relaxation is attributed partially to the different glass transition temperature of blend components (Fox–Flory equation for blends) and partially to the restriction of mobility in the amorphous phase of a semi-crystalline matrix caused by the addition of dendrimers. This is further supported by the results of a dielectric study of hyperbranched aromatic polyamide and polyamide-6,6 blends [39] where the increase in the glass transition temperature with increasing concentration of the hyperbranched polymer was explained by a decreased mobility of polyamide chains in the amorphous phase.

3.2.2. Dynamic mechanical spectroscopy (DMS)

The results of dynamic mechanical spectroscopy (DMS) are discussed next. The storage and loss moduli in the frequency domain for the neat PPO and its blends with generation 0 at 218 K are shown in Fig. 12. The data were shifted horizontally with respect to the reference curves at 218 K. It can be seen that the viscoelastic response in segmental and terminal zone does not change with dendrimer concentration. In the terminal relaxation zone the storage modulus (G') and the loss modulus (G'') scale with frequency to the power of 2 and 1, respectively, as shown in Fig. 12. Thus dendrimer blends exhibit the characteristic response of a linear viscoelastic polymer. The average relaxation time for the segmental and the normal mode processes, obtained from the HN fits does not change with respect to the neat PPO. The spectral breadth and symmetry parameters for segmental and normal mode relaxations are independent of temperature. Analogous results

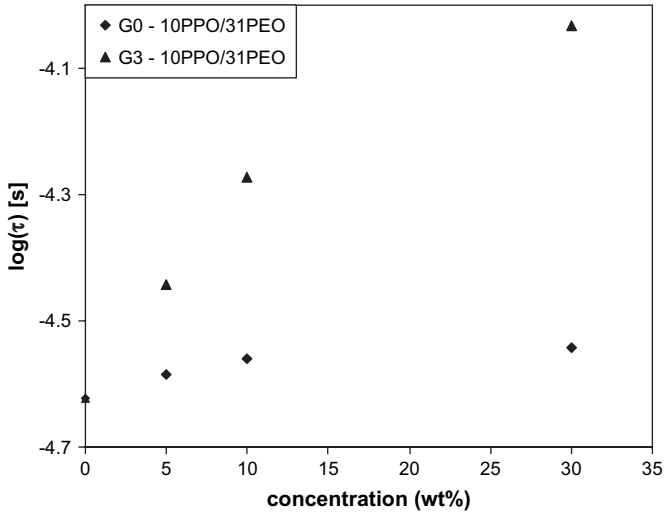

Fig. 11. Average relaxation time for the segmental process in PAMAM–10PPO/31PEO blends as a function of dendrimer concentration at 223 K.

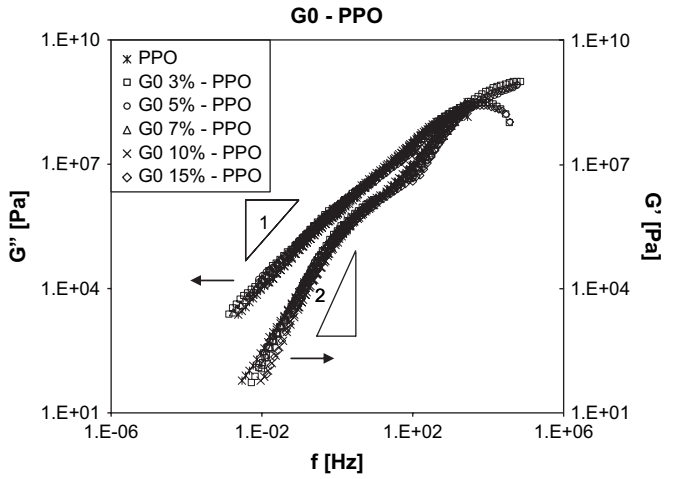

Fig. 12. Storage (G') and loss (G'') moduli in the frequency domain in PAMAM–PPO blends with G0 concentration as a parameter at 218 K.

were observed for PPO blends with generation 3, as well as for blends with generations 0 and 3 in the 29PPO/6PEO matrix, but those data are not presented. We recall that the DRS spectra reveal a slight shift of normal and segmental mode to higher frequency with increasing concentration of generation 3 dendrimers in blends with PPO, but the absence of such change in the DMS spectra is not surprising because dynamic mechanical spectroscopy is not sensitive to molecular architecture in the same way that dielectric relaxation spectroscopy is [25]. Apart from this difference, the combined results of DMS and DRS analyses yield the following observations: (1) the average relaxation times for segmental and normal mode follow the same general trend with temperature, and (2) the time scales of these processes obtained by DRS and DMS are in good agreement.

4. Conclusions

In this work we have described the effect of hydrophilicity and morphological characteristics of three types of polymer matrices, a homopolymer (PPO) and two block copolymers (PPO/PEO) on the molecular dynamics of their blends with generation 0 or 3 PAMAM dendrimers. We acknowledge that generation 0 is not a fully developed dendrimer although it is a precursor for all subsequent generations. Dynamics were studied by dielectric relaxation spectroscopy (DRS) and dynamic mechanical spectroscopy (DMS) over a wide range of frequencies and temperatures. The key conclusions are as follows.

PPO and 29PPO/6PEO are amorphous polymers that display both segmental and normal mode relaxations. Interestingly, the normal mode process, due to the global motions of PPO chains, is slower in the block copolymer. We interpret this finding as the result of an increase in the end-to-end distance of hydrophobic PPO chains upon the introduction of the incompatible hydrophilic PEO block. The 10PPO/31PEO block copolymer is crystalline and it shows only one relaxation process associated with the segmental motions within the amorphous phase.

Interesting observations were made about the time scale of the segmental process in the blends. A slight decrease in the time scale was found in the PAMAM–PPO blends and we ascribed this result to the fact that dendrimers act as hard-sphere diluents in the PPO matrix by decreasing the self-association of PPO chains and consequently promoting their mobility. In the 29PPO/6PEO matrix, the time scale of segmental relaxation is independent of dendrimer concentration, while in the more morphologically complex (10PPO/31PEO) matrix, the time scale increases with increasing dendrimer concentration. We assign the observed increase in the relaxation time to the addition of dendrimers to the amorphous phase where they further restrict chain mobility.

DMS results reveal no change in the storage and loss moduli in the blends with respect to the neat polymers. All blends are marked by the characteristic terminal zone response, where the slopes of G' and G'' scale with frequency to the power of 2 and 1, respectively. A direct comparison of DMS and DRS results shows that the average relaxation times for segmental and normal mode relaxations follow the same general trend with respect to temperature. The time scales of relaxation determined from DRS and DMS spectra are in good agreement and the relaxation spectra are thermodielectrically and thermorheologically simple.

Acknowledgement

This material is based on the work supported by National Science Foundation under Grant DMR-0346435.

References

[1] Fréchet JMJ, Tomalia DA. Dendrimers and other dendritic polymers. West Sussex, England: Wiley; 2001.
[2] Newkome GR, Moorefield CN, Vogtle F. Dendrimers and dendrons: concept, synthesis, applications. Weinheim: Wiley-VCH; 2001.
[3] Bosman AW, Janssen HM, Meijer EW. Chem Rev 1999;99(7):1665–88.
[4] Buhleier E, Wehner W, Vogtle F. Synthesis 1978:155–8.
[5] Denkewalter RG, Kolc J, Lukasavage WJ. US Patent 4,289,872; 1981.
[6] Newkome GR, Yao Z, Baker GR, Gupta VK. J Org Chem 1985;50:2003–4.
[7] Tomalia DA, Baker H, Dewald J, Hall M, Kallos G, Martin S, et al. Polym J 1985;17:117–32.
[8] Hawker CJ, Fréchet JMJ. J Am Chem Soc 1990;112:7638–47.
[9] Wiener E, Brechbiel MW, Brothers H, Magin RL, Gansow OA, Tomalia DA, et al. Magn Reson Med 1994;31(1):1–8.
[10] Venditto VJ, Regino CA, Brechbiel MW. Mol Pharm 2005;2(4):302–11.
[11] Myc A, Majoros IJ, Thomas TP, Baker Jr JR. Biomacromolecules 2007;8(1):13–8.
[12] Ispasoiu RG, Balogh L, Varnavski OP, Tomalia DA, Goodson T. J Am Chem Soc 2000;122(44):11005–6.
[13] Crooks RM, Zhao M, Sun L, Chechik V, Yeung LK. Acc Chem Res 2001;34(3):181–90.
[14] Dufes C, Uchegbu IF, Schatzlein AG. Adv Drug Deliv Rev 2005;57(15):2177–202.
[15] Esfand R, Tomalia DA. Drug Discov Today 2001;6(8):427–36.
[16] Gillies ER, Frèchet JMJ. Drug Discov Today 2005;10(1):35–43.
[17] Uppuluri S, Morrison FA, Dvornic PR. Macromolecules 2000;33(7):2551–60.
[18] Williams G. Dielectric relaxation spectroscopy of amorphous polymer systems: the modern approach. In: Riande E, editor. Keynote lectures in polymer science. Madrid: CSIC; 1995.
[19] Riande E, Diaz-Calleja R. Electrical properties of polymers. New York: Marcel Dekker; 2004.
[20] Dantras E, Lacabanne C, Caminade AM, Majoral JP. Macromolecules 2001;34(12):3808–11.
[21] Dantras E, Caminade AM, Majoral JP, Lacabanne C. J Phys D Appl Phys 2002;35:5–8.
[22] Dantras E, Dandurand J, Lacabanne C, Caminade AM, Majoral JP. Macromolecules 2004;37(8):2812–6.
[23] Trahasch B, Stuhn B, Frey H, Lorenz K. Macromolecules 1999;32(6):1962–6.
[24] Trahasch B, Frey H, Lorenz K, Stuhn B. Colloid Polym Sci 1999;277(12):1186–92.
[25] Mijovic J, Ristic S, Kenny J. Macromolecules 2007;40(14):5212–21.
[26] Fitz B, Andjelic S, Mijovic J. Macromolecules 1997;30(18):5227–38.
[27] Kremer F, Schönhals A, editors. Broadband dielectric spectroscopy. Berlin: Springer-Verlag; 2002.
[28] McCrum NG, Read BE, Williams G. Anelastic and dielectric effects in polymeric solids. London: Wiley; 1967.
[29] Havriliak SJ, Negami S. Polymer 1967;8:161–210.
[30] Mijovic J, Sun M, Han Y. Macromolecules 2002;35(16):6417–25.
[31] Mijovic J, Han Y, Sun M, Pejanovic S. Macromolecules 2003;36(12):4589–602.
[32] Stockmayer WH. Pure Appl Chem 1967;15:539.
[33] Sy JW, Mijovic J. Macromolecules 2000;33(3):933–46.
[34] Mijovic J, Sy JW, Kwei TK. Macromolecules 1997;30(10):3042–50.
[35] Nicolai T, Floudas G. Macromolecules 1998;31(8):2578–85.
[36] Nicolai T, Prochazka F, Durand D. Phys Rev Lett 1999;82(4):863–6.
[37] Cole RH, Cole KS. J Chem Phys 1942;10:98–105.
[38] Bian Y, Pejanovic S, Kenny J, Mijovic J. Macromolecules 2007;40(17):6239–48.
[39] Hakme C, Stevenson I, Fulchiron R, Seytre G, Clement F, Odoni L, et al. J App Polym Sci 2005;97(4):1522–37.